We are IntechOpen, the world's leading publisher of Open Access books Built by scientists, for scientists

4,800
Open access books available

122,000
International authors and editors

135M
Downloads

Our authors are among the

154
Countries delivered to

TOP 1%
most cited scientists

12.2%
Contributors from top 500 universities

CLARIVATE ANALYTICS BOOK CITATION INDEX INDEXED

WEB OF SCIENCE™

Selection of our books indexed in the Book Citation Index in Web of Science™ Core Collection (BKCI)

Interested in publishing with us?
Contact book.department@intechopen.com

Numbers displayed above are based on latest data collected.
For more information visit www.intechopen.com

6

Modeling and Motion Control Strategy for AUV

Lei Wan and Fang Wang
Harbin Engineering University
China

1. Introduction

Autonomous Underwater Vehicles (AUV) speed and position control systems are subjected to an increased focus with respect to performance and safety due to their increased number of commercial and military application as well as research challenges in past decades, including underwater resources exploration, oceanographic mapping, undersea wreckage salvage, cable laying, geographical survey, coastal and offshore structure inspection, harbor security inspection, mining and mining countermeasures (Fossen, 2002). It is obvious that all kinds of ocean activities will be greatly enhanced by the development of an intelligent underwater work system, which imposes stricter requirements on the control system of underwater vehicles. The control needs to be intelligent enough to gather information from the environment and to develop its own control strategies without human intervention (Yuh, 1990; Venugopal and Sudhakar, 1992).

However, underwater vehicle dynamics is strongly coupled and highly nonlinear due to added hydrodynamic mass, lift and drag forces acting on the vehicle. And engineering problems associated with the high density, non-uniform and unstructured seawater environment, and the nonlinear response of vehicles make a high degree of autonomy difficult to achieve. Hence six degree of freedom vehicle modeling and simulation are quite important and useful in the development of undersea vehicle control systems (Yuh, 1990; Fossen 1991, Li et al., 2005). Used in a highly hazardous and unknown environment, the autonomy of AUV is the key to work assignments. As one of the most important subsystems of underwater vehicles, motion control architecture is a framework that manages both the sensorial and actuator systems (Gan et al., 2006), thus enabling the robot to undertake a user-specified mission.

In this chapter, a general form of mathematical model for describing the nonlinear vehicle systems is derived, which is powerful enough to be applied to a large number of underwater vehicles according to the physical properties of vehicle itself to simplify the model. Based on this model, a simulation platform "AUV-XX" is established to test motion characteristics of the vehicle. The motion control system including position, speed and depth control was investigated for different task assignments of vehicles. An improved S-surface control based on capacitor model was developed, which can provide flexible gain selections with clear physical meaning. Results of motion control on simulation platform "AUV-XX" are described.

2. Mathematical modeling and simulation

Six degree of freedom vehicle simulations are quite important and useful in the development of undersea vehicle control systems. There are several processes to be modeled in the simulation including the vehicle hydrodynamics, rigid body dynamics, and actuator dynamics, etc.

2.1 AUV kinematics and dynamics

The mathematical models of marine vehicles consist of kinematic and dynamic part, where the kinematic model gives the relationship between speeds in a body-fixed frame and derivatives of positions and angles in an Earth-fixed frame, see Fig.1. The vector of positions and angles of an underwater vehicle $\eta = [x, y, z, \varphi, \theta, \psi]^T$ is defined in the Earth-fixed coordinate system(E) and vector of linear and angular v $v = [u, v, w, p, q, r]^T$ elocities is defined in a body-fixed(B) coordinate system, representing surge, sway, heave, roll, pitch and yaw velocity, respectively.

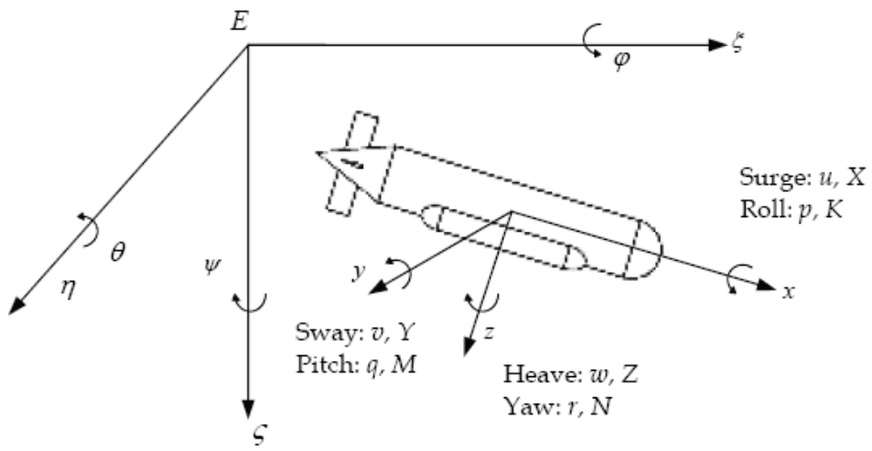

Fig. 1. Earth-fixed and body-fixed reference frames

According to the Newton-Euler formulation, the 6 DOF rigid-body equations of motion in the body-fixed coordinate frame can be expressed as:

$$\begin{cases} m\left[(\dot{u}_r - v_r r + w_r q) - x_G(q^2 + r^2) + y_G(pq - \dot{r}) + z_G(pr + \dot{q})\right] = X \\ m\left[(\dot{v}_r - w_r p + u_r r) - y_G(r^2 + p^2) + z_G(qr - \dot{p}) + x_G(qp + \dot{r})\right] = Y \\ m\left[(\dot{w}_r - u_r q + v_r p) - z_G(p^2 + q^2) + x_G(rp - \dot{q}) + y_G(rq + \dot{p})\right] = Z \\ I_x\dot{p} + (I_z - I_y)qr + m\left[y_G(\dot{w}_r + pv_r - qu_r) - z_G(\dot{v}_r + ru_r - pw_r)\right] = K \\ I_y\dot{q} + (I_x - I_z)rp + m\left[z_G(\dot{u}_r + w_r q - v_r r) - x_G(\dot{w}_r + pv_r - u_r q)\right] = M \\ I_z\dot{r} + (I_y - I_z)pq + m\left[x_G(\dot{v}_r + u_r r - pw_r) - y_G(\dot{u}_r + qw_r - v_r r)\right] = N \end{cases} \quad (1)$$

where m is the mass of the vehicle, I_x, I_y and I_z are the moments of inertia about the x_b, y_b and z_b -axes, x_g, y_g and z_g are the location of center of gravity, u_r, v_r, w_r are relative

translational velocities associated with surge, sway and heave to ocean current in the body-fixed frame, here assuming the sea current to be constant with orientation in yaw only, which can be described by the vector $\boldsymbol{U}_c = [u_c, v_c, w_c, 0, 0, \alpha_c]^{\mathrm{T}}$. The resultant forces X, Y, Z, K, M, N includes positive buoyant $B - W = \Delta P$ (since it is convenient to design underwater vehicles with positive buoyant such that the vehicle will surface automatically in the case of an emergency), hydrodynamic forces $X_H, Y_H, Z_H, K_H, M_H, N_H$ and thruster forces.

2.2 Thrust hydrodynamics modeling

The modeling of thruster is usually done in terms of advance ratio J_0, thrust coefficients K_T and torque coefficient K_Q. By carrying out an open water test or a towing tank test, a unique curve where J_0 is plotted against K_T and K_Q can be obtained for each propeller to depict its performance. And the relationship of the measured thrust force versus propeller revolutions for different speeds of advance is usually least-squares fitting to a quadratic model.

Here we introduce a second experimental method to modeling thruster dynamics. Fig.2 shows experimental results of thrusters from an open water test in the towing tank of the Key Lab of Autonomous Underwater Vehicles in Harbin Engineering University. The results are not presented in the conventional way with the thrust coefficient K_T plotted versus the open water advance coefficient J_0, for which the measured thrust is plotted as a function of different speeds of vehicle and voltages of the propellers.

The thrust force of the specified speed of vehicle under a certain voltage can be finally approximated by Atiken interpolation twice. In the first interpolation, for a certain voltage, the thrust forces with different speeds of the vehicle (e.g. 0m/s, 0.5m/s, 1.0m/s, 1.5m/s) can be interpolated from Fig.1, and plot it versus different speeds under a certain voltage. Then based on the results of the first interpolation, for the second Atiken interpolation we can find the thrust force for the specified speed of the vehicle.

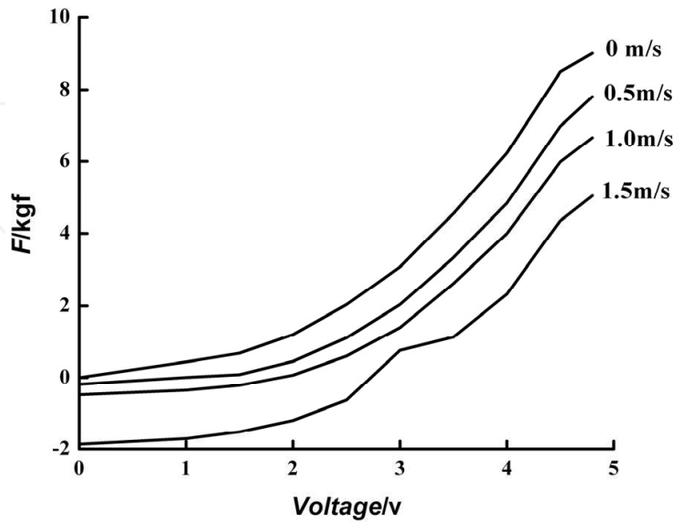

Fig. 2. Measured thrust force as a function of propeller driving voltage for different speeds of vehicle

Compared with conventional procedure to obtain thrust that is usually done firstly by linear approximating or least-squares fitting to K_T - J_0 plot (open water results), then using formulation $F_t = K_t n^2 D^4$ to compute the thrust F_t . The experimental results of open water can be directly used to calculate thrust force without using the formulation, which also can be applied to control surface of rudders or wings, *etc*.

2.3 General dynamic model

To provide a form that will be suitable for simulation and control purposes, some rearrangements of terms in Eq.(1) are required. First, all the non-inertial terms which have velocity components were combined with the fluid motion forces and moments into a fluid vector denoted by the subscript vis (viscous). Next, the mass matrix consisting all the coefficient of rigid body's inertial and added inertial terms with vehicle acceleration components $\dot{u},\dot{v},\dot{w},\dot{p},\dot{q},\dot{r}$ was defined by matrix $\boldsymbol{E}$, and all the remaining terms were combined into a vector denoted by the subscript else, to produce the final form of the model:

$$\boldsymbol{E}\dot{\boldsymbol{X}} = \boldsymbol{F}_{\text{vis}} + \boldsymbol{F}_{\text{else}} + \boldsymbol{F}_t \tag{2}$$

where $\boldsymbol{X} = [u,v,w,p,q,r]^{\text{T}}$ is the velocity vector of vehicle with respect to the body-fixed frame.

Hence, the 6 DOF equations of motion for underwater vehicles yield the following general representation:

$$\begin{cases} \dot{\boldsymbol{X}} = \boldsymbol{E}^{-1}(\boldsymbol{F}_{\text{vis}} + \boldsymbol{F}_{\text{else}} + \boldsymbol{F}_t) \\ \dot{\boldsymbol{\eta}} = \boldsymbol{J}(\eta)\boldsymbol{X} \end{cases} \tag{3}$$

with

$$\boldsymbol{E} = \begin{bmatrix} m-X_{\dot{u}} & 0 & 0 & 0 & mz_G & -my_G \\ 0 & m-Y_{\dot{v}} & 0 & -mz_G-Y_{\dot{p}} & 0 & mx_G-Y_{\dot{r}} \\ 0 & 0 & m-Z_{\dot{w}} & my_G & -mx_G-Z_{\dot{q}} & 0 \\ 0 & -mz_G-K_{\dot{v}} & 0 & I_x-K_{\dot{p}} & 0 & -K_{\dot{r}} \\ mz_G & 0 & -mx_G-M_{\dot{w}} & 0 & I_y-M_{\dot{q}} & 0 \\ 0 & mx_G-N_{\dot{v}} & 0 & -N_{\dot{p}} & 0 & I_z-N_{\dot{r}} \end{bmatrix} \tag{4}$$

where $\boldsymbol{J}(\eta)$ is the transform matrix from body-fixed frame to earth-fixed frame, η is the vector of positions and attitudes of the vehicle in earth-fixed frame.

The general dynamic model is powerful enough to apply it to different kinds of underwater vehicles according to its own physical properties, such as planes of symmetry of body, available degrees of freedom to control, and actuator configuration, which can provide an effective test tool for the control design of vehicles.

3. Motion control strategy

In this section, the design of motion control system of AUV-XX is described. The control system can be cast as two separate designs, which include both position and speed control

in horizontal plane and the combined heave and pitch control for dive in vertical plane. And an improved S-surface control algorithm based on capacitor plate model is developed.

3.1 Control algorithm

As a nonlinear function method to construct the controller, S-surface control has been proven quite effective in sea trial for motion control of AUV in Harbin Engineering University (Li et al., 2002). The nonlinear function of S-surface is given as:

$$u = 2.0/(1.0 + \exp(-k_1 e - k_2 \dot{e})) - 1.0 \tag{5}$$

where $e, \dot{e}$ are control inputs, and they represent the normalized error and change rate of the error, respectively; u is the normalized output in each degree of freedom; k_1, k_2 are control parameters corresponding to control inputs e and $\dot{e}$ respectively, and we only need to adjust them to meet different control requirements.

Based on the experiences of sea trials, the control parameters k_1, k_2 can be manually adjusted to meet the fundamental control requirements, however, whichever combination of k_1, k_2 we can adjust, it merely functions a global tuning which dose not change control structure. Here the improved S-surface control algorithm is developed based on the capacitor with each couple of plates putting restrictions on the control variables $e, \dot{e}$ respectively, which can provide flexible gain selection with proper physical meaning.

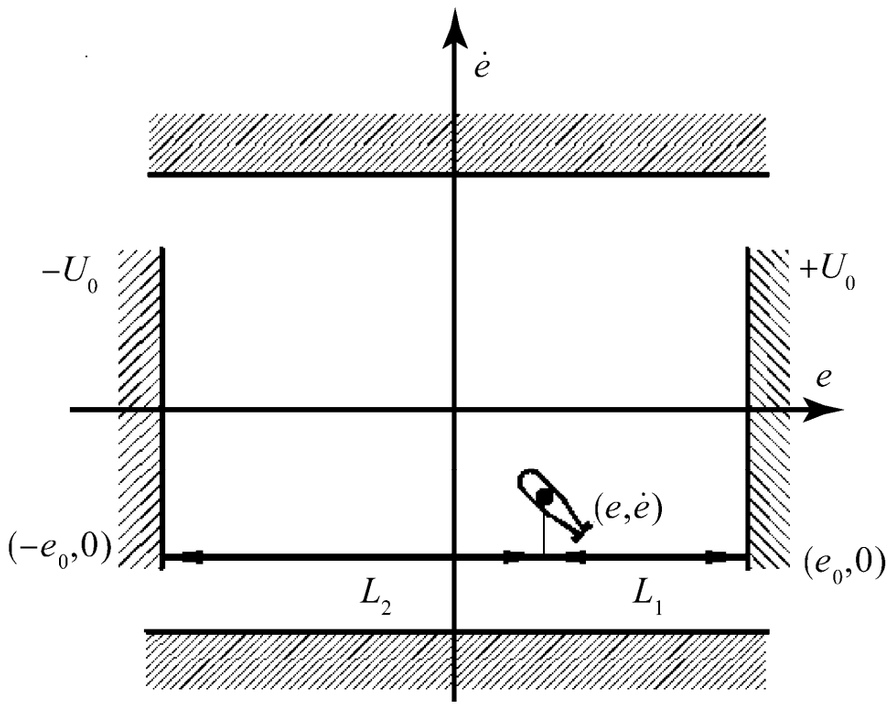

Fig. 3. Capacitor plate model

The capacitor plate model as shown in Fig.3 demonstrates the motion of a charged particle driven by electrical field in capacitor is coincident with the motion of a controlled vehicle from current point $(e,\dot{e})$ to the desired point, for which the capacitor plate with voltage

serves as the controller, and the equilibrium point of electrical field is the desired position that the vehicle is supposed to reach.
Due to the restriction of two couples of capacitor plates put on control variables e and $\dot{e}$, the output of model can be obtained as

$$y = u^{+U_0} + u^{-U_0} = F(L_1, L_2)(+U_0) + F(L_2, L_1)(-U_0) \tag{6}$$

where L_1, L_2 are horizontal distances from the current position of the vehicle to each capacitor plate, respectively, and the restriction function $F(*,*)$ is defined to be hyperbolic function of L_1, L_2 by Ren and Li (2005):

$$\begin{cases} F(L_1, L_2) = \dfrac{L_1^{-k}}{L_1^{-k} + L_2^{-k}} \\ F(L_2, L_1) = \dfrac{L_2^{-k}}{L_1^{-k} + L_2^{-k}} \end{cases} \tag{7}$$

The restriction function $F(*,*)$ reflects the closer the current position $(e, \dot{e})$ of vehicle moving to capacitor plate, the stronger the electrical field is. Choosing $U_0 = 1$, the output of capacitor plate model yields:

$$u = \frac{L_1^{-k} - L_2^{-k}}{L_1^{-k} + L_2^{-k}} U_0 = \frac{(e_0 + e)^k - (e_0 - e)^k}{(e_0 + e)^k + (e_0 - e)^k} \tag{8}$$

where e_0 is the distance between the plate and field equilibrium point of capacitor.
An improved S-surface controller based on the capacitor plate model is proposed, that is

$$\begin{cases} u_{ei} = [2.0 \Big/ \left(1.0 + (\dfrac{e_0 - e_i}{e_0 + e_i})^{ki1} \right) - 1.0] \\ u_{\dot{e}i} = [2.0 \Big/ \left(1.0 + (\dfrac{e_0 - \dot{e}_i}{e_0 + \dot{e}_i})^{ki2} \right) - 1.0] \\ f_i = K_{ei} \cdot u_{ei} + K_{\dot{e}i} \cdot u_{\dot{e}i} \end{cases} \tag{9}$$

where f_i is the outputted thrust force of controller for each DOF, and $K_{ei} = K_{\dot{e}i} = K_i$ is the maximal thrust force in i th DOF, therefore the control output can be reduced to

$$\begin{cases} u_i = u_{ei} + u_{\dot{e}i} = [2.0 \Big/ \left(1.0 + (\dfrac{e_0 - e_i}{e_0 + e_i})^{ki1} \right) - 1.0] + [2.0 \Big/ \left(1.0 + (\dfrac{e_0 - \dot{e}_i}{e_0 + \dot{e}_i})^{ki2} \right) - 1.0] \\ f_i = K_i \times u_i \end{cases} \tag{10}$$

The capacitor model's S-surface control can provide flexible gain selections with different forms of restriction function to L_1, L_2 to meet different control requirements for different phases of control procedure.

3.2 Speed and position control in horizontal plane

Since AUV-XX is equipped with two transverse tunnel thrusters in the vehicle fore and aft respectively and two main thrusters (starboard and port) aft in horizontal plane, which can produce a force in the *x*-direction needed for transit and a force in the *y*-direction for maneuvering, respectively. So both speed and position controllers are designed in horizontal plane.

Speed control is to track the desired surge velocity with fixed yaw angle and depth, which is usually used in long distance transfer of underwater vehicles. Before completing certain kind of undersea tasks, the vehicle needs to experience long traveling to achieve the destination. In this chapter, speed control is referred to a forward speed controller in surge based on the control algorithm we introduced in above section, its objective is to make the vehicle transmit at a desired velocity with good and stable attitudes such as fixed yaw and depth.

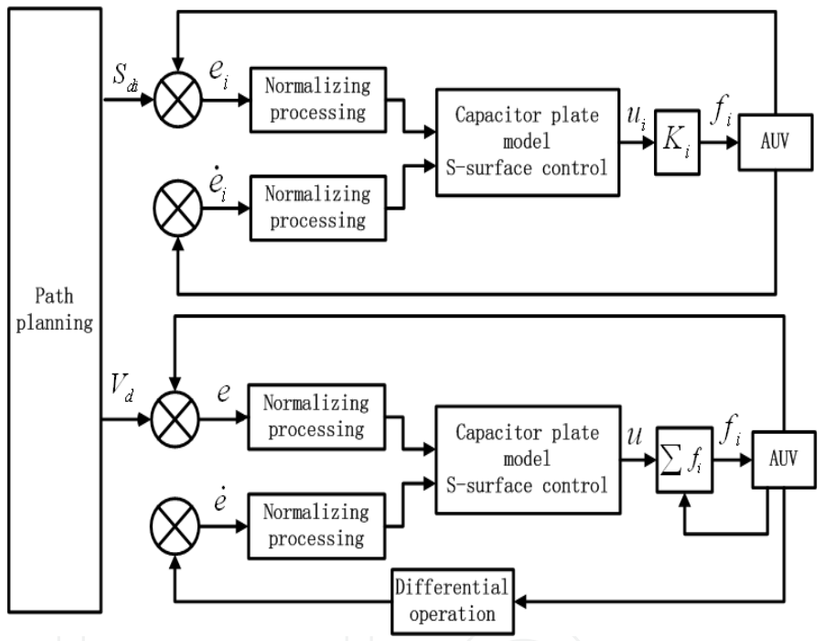

Fig. 4. Position and speed control loop

Position control enables the vehicle to perform various position-keeping functions, such as maintaining a steady position to perform a particular task, following a prescribed trajectory to search for missing or seek after objects. Accurate position control is highly desirable when the vehicle is performing underwater tasks such as cable laying, dam security inspection and mine clearing. To ensure AUV-XX to complete work assignments of obstacles avoiding, target recognition, and mine countermeasures, we design position controllers for surge, sway, yaw and depth respectively for equipping the vehicle with abilities of diving at fixed deepness, navigating at desired direction, sailing to given points and following the given track, *etc*.

As for the desired or target position or speed in the control system, it is the path planning system who decides when to adopt and switch control scheme between position and speed, the desired position that the vehicle is supposed to reach, and the velocity at which the

vehicle should navigate with respect to the present tasks and motion states of the vehicle as well as operation environment.

Fig.4 shows both position and speed control procedures. It can be seen that it is easier to realize the control algorithm. For position control of i th DOF, the control inputs are the position error and the change rate of position error, that is the velocity obtained from motion sensors; while for speed control, the velocity error and acceleration are control inputs, since AUV-XX is not equipped with IGS to acquire the acceleration of the vehicle, acceleration is calculated differential the velocity in each control step.

3.3 Combined control of pitch and heave in vertical plane

Since when the vehicle is moving at a high speed, the thrust that tunnel thrusters can provide will strongly degrade, it is difficult to control the depth merely using tunnel thrusters. Considering that once the depth or height of the vehicle changes, the pitch will change with it, and vice versa, so we combine pitch with heave control for diving when the vehicle is moving at some high speed to compensate for the thrust reduction of tunnel thrusters. In that case, the desired pitch angle can be designed as a function of the surge velocity of the vehicle:

$$\theta_T = \begin{cases} -\dfrac{k_\theta \cdot \Delta z}{\sqrt{u}} - \theta_0 & u \geq 0.8m/s \\ 0 & u < 0.8m/s \end{cases} \tag{11}$$

where θ_T is the target pitch angle, k_θ is a positive parameter to be adjusted, Δz is the depth deviation, u is the surge velocity of vehicle, θ_0 is the pitch angle when the vehicle is in static equilibrium. Since the change of pitch angle is usually associated with depth change and they affect each other, the target pitch is the output of the proportional control with respect to depth change with the proportional parameters k_θ, the velocity threshold of 0.8m/s is chosen based on the engineering experience of the sea trial and the capability of the thruster system of the vehicle.

When the vehicle is moving at a low speed($u < 0.8m/s$), tunnel thrusters can normally provide the needed force, so the command of target pitch will not be sent to motion control. According to control law (9), we can get the output of the heave controller. Since the vehicle is usually designed with positive buoyancy, the final output of control of heave can be obtained by

$$f_3 = K_3 \cdot u_3 + \Delta P \tag{12}$$

where ΔP is the positive buoyancy.

And as the surge velocity grows, the thrust of vertical tunnel will experience worse reduction and degradation, so the role it plays in the depth control will be greatly abridged, as a result, the output of pitch control of the main vertical thrusters aft of the vehicle should compensate for that, so the output of control will finally yields as

$$f_5 = \begin{cases} K_5 u_5 & u \leq 0.8 \\ K_5(\varepsilon_1 \cdot u_3 + \varepsilon_2 \cdot u_5) & u > 0.8 \end{cases} \tag{13}$$

with

$$\begin{cases} \varepsilon_1 = \alpha_1 / \sqrt{\beta u} \\ \varepsilon_2 = \alpha_2 \cdot \exp(u \cdot u / 10) \end{cases} \tag{14}$$

where $\alpha_1, \alpha_2, \beta$ can be manually adjusted based on experiences. The block diagram of combined control of pitch and depth in vertical plane can be in Fig.5.

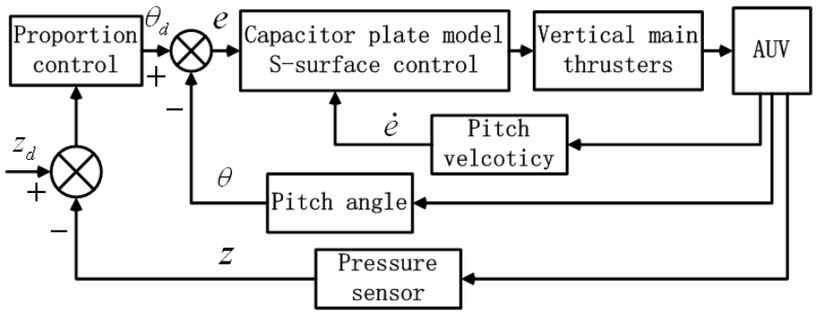

Fig. 5. Combined control of pitch and depth in vertical plane

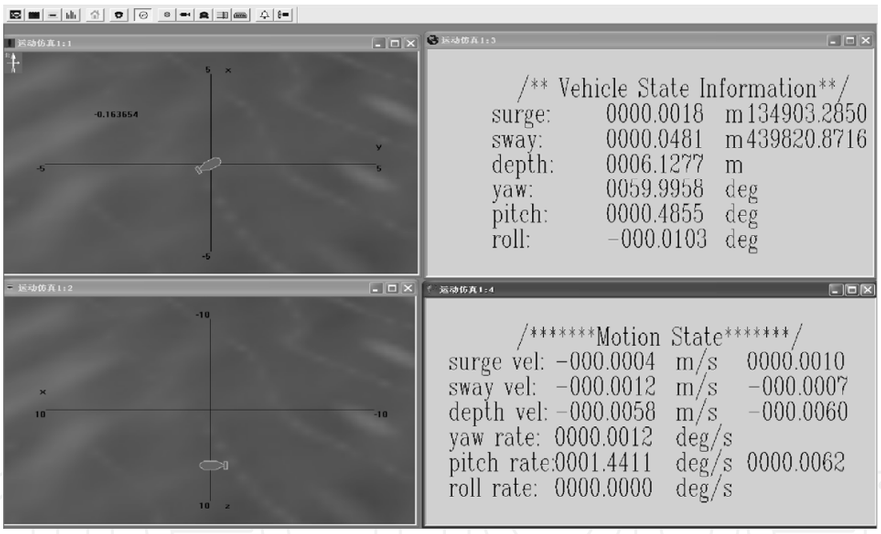

Fig. 6. AUV-XX simulation platform

4. Simulation results and analysis

To verify the feasibility and effectiveness of the motion control system for the vehicle AUV-XX, simulations are carried out in the AUV-XX simulation platform. The vehicle researched in this chapter named by AUV-XX, AUV-XX's configuration is basically a long cylinder of 0.5m in diameter and 5m in length with crossed type wings near its rear end. On each edge of the wings, a thruster is mounted, which is used for both turn and dive. AUV-XX is also equipped with a couple of lateral tunnel thrusters for sway and a couple of vertical tunnel thrusters fore and aft of the vehicle, respectively. Based on the modeling method described in above section, we established the AUV-XX simulation platform to carry out fundamental

tests on its motion characteristics, stability and controllability. The states of the vehicle including positions, attitudes and velocities are obtained at each instant by solving the mathematical model equation by integration using a time step of 0.5s. Fig.6 shows the interface of AUV-XX simulation platform. Fig.7 shows the data flow of the simulation platform connecting with motion control system.

Figs.8–10 show the simulation results of capacitor plate model's S-surface control for separate position and speed control in surge, sway and yaw respectively, and also combined control of heave and pitch for diving of the vehicle. The roll is left uncontrolled. And all the vehicle states, including speed, are initialized to zero at the beginning of the each of the simulation. The solid lines denote the actual responses of the vehicle while the dashed denote the desired position or speed that the vehicle is commanded to achieve.

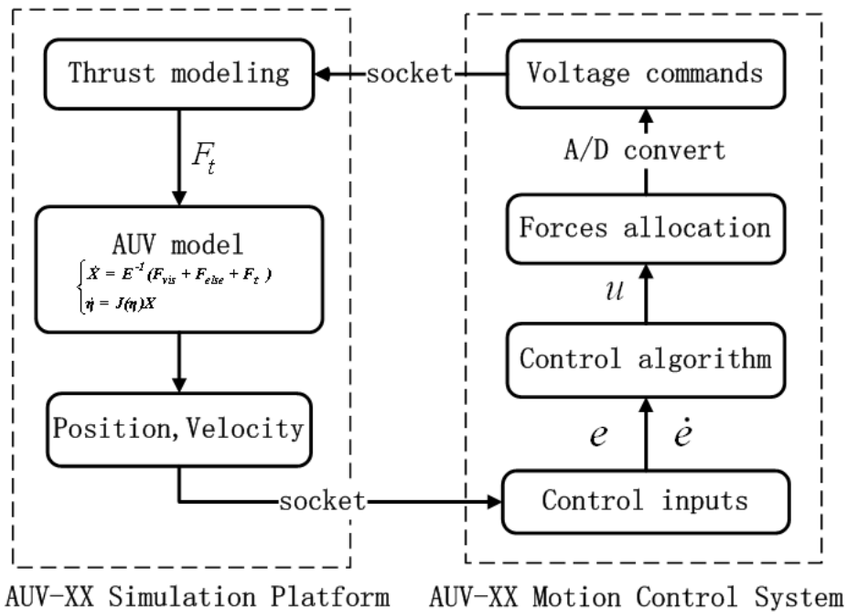

Fig. 7. Data flow of AUV-XX motion control in simulation platform

It can be seen from Fig.8 that, the vehicle is commanded to move to some specified positions in surge, sway and yaw, respectively. For the case of surge as shown in Fig.8(a) and Fig.8(b), the larger position deviation from the target position produces faster response of surge velocity. Compared with responses of surge and yaw, the sway is slower with a rise time of 150s for the desired position is 16m, which may result from that the lateral resistance is much larger longitudinally and the thrust of transverse tunnel thrusters can provide is smaller than the main aft thrusters.

Fig.9 shows the speed control results of surge with constant yaw and depth keeping. The desired velocity is 1m/s and once the vehicle is moving stably with such speed then the vehicle is commanded to track the specified depth (5m) and yaw (45^o) commands. It can be seen that there is no overshoot in surge speed and system response is fast with the yaw experiencing an accepted overshoot of $\pm 2^o$, and the depth is stably maintained, hence the vehicle is able to move at a desired speed with a desired fixed heading and depth. The speed control simulation results prove the feasibility of the proposed speed control strategy.

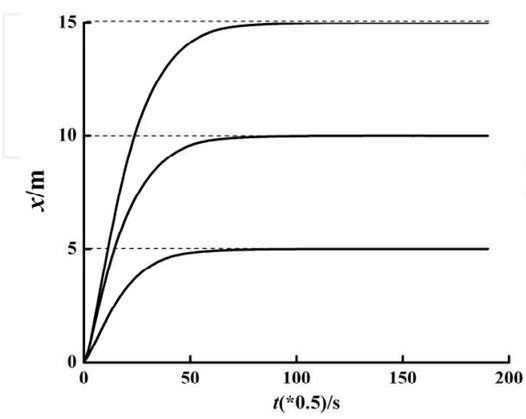

(a) Surge displacement

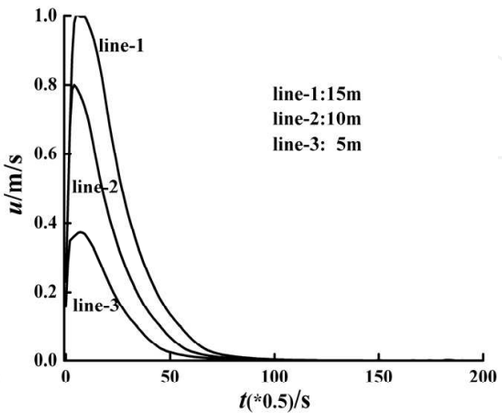

(b) Surge velocity response

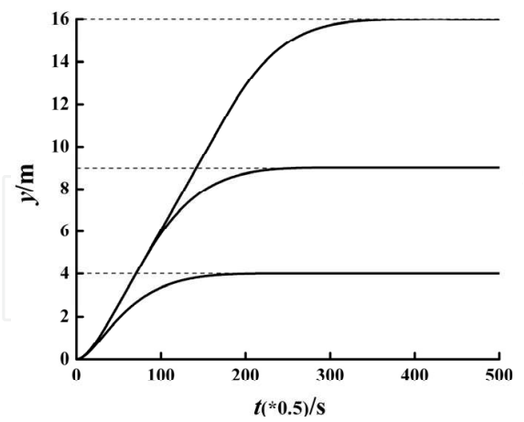

(c) Sway displacement

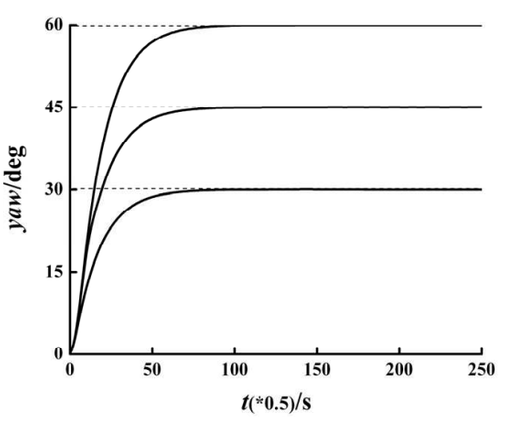

(d) Yaw displacement

Fig. 8. Position control results of surge, sway and yaw

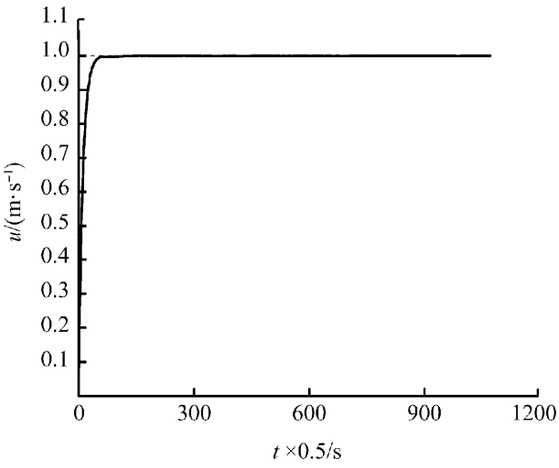

(a) Surge speed response

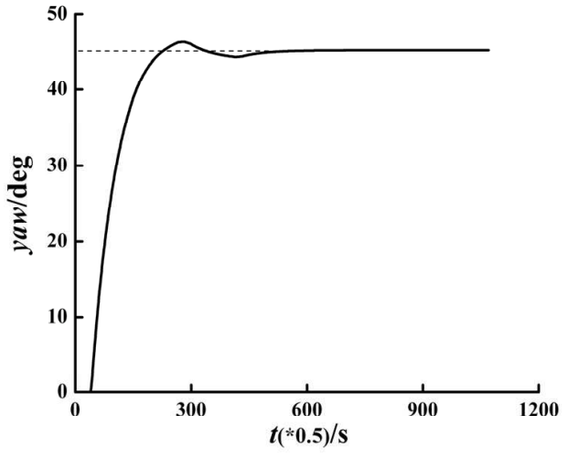

(b) Yaw keep response

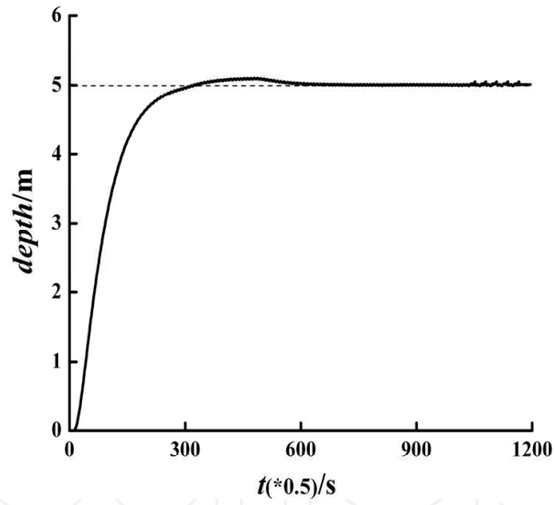

(c) Depth keep response

Fig. 9. Speed control results of surge with yaw and depth keeping

Fig.10 shows the combined control of heave and pitch for diving in vertical plane. For this case, the velocity of surge that the vehicle is commanded to track is 1.5m/s, which is not very large so that the vertical tunnel thrusters will suffer thrust reduction to some extent but still can work to provide a portion of vertical thrust for diving. Hence when the vehicle is commanded to dive, the pitch will not experience a large change, which is reasonable design consideration in the case of large inertial vehicles.

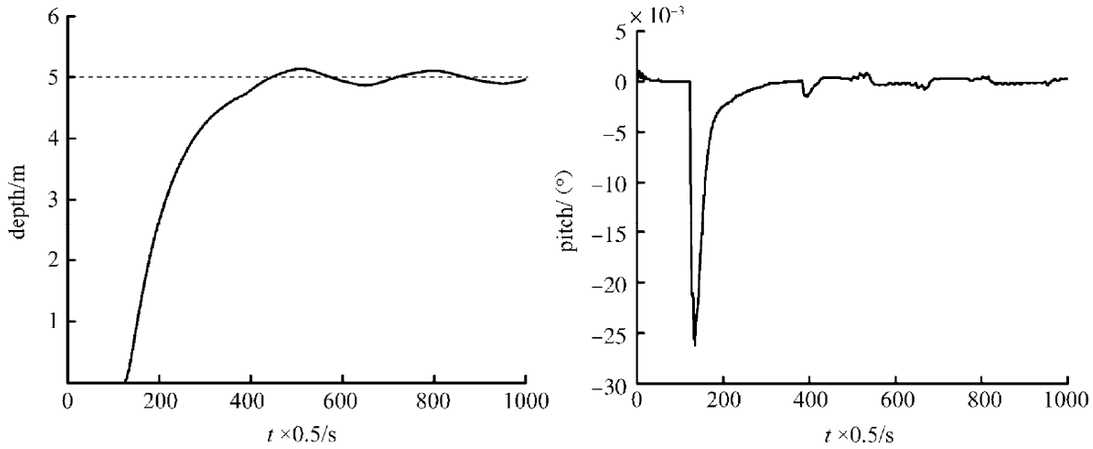

(c) Depth keep response (d) Pitch response

Fig. 10. Combined depth control of heave and pitch

5. Conclusions

In this chapter, the design of motion control system for Autonomous Underwater Vehicles is described, which includes both position and speed control in horizontal plane and combined control of heave and pitch in vertical plane. To construct the control system, a 6 DOF general mathematical model of underwater vehicles was derived, which is powerful enough to apply it to different kinds of underwater vehicles according to its own physical properties. Based on the general mathematical model, a simulation platform was established to test motion characteristics, stability and controllability of the vehicle. To demonstrate the performance of the designed controller, simulations have been carried out on AUV-XX simulation platform and the capacitor plate model S-surface control shows a good performance.

6. References

Fossen T. I. (1991). *Nonlinear modeling and control of underwater vehicles*. Ph.D. thesis, Norwegian Institute of Technology-NTH, Trondheim, Norway

Fossen T. I. (2002). *Marine control system*: *guidance*, *navigation and control of ships*, *rigs and underwater vehicles*. Marine Cybernetics, Trondheim, 254-260

Gan Yong, Sun Yushan, Wan Lei, Pang Yongjie (2006). Motion control system architecture of underwater robot. *Proceedings of the 6th World Congress on Intelligent Control and Automation*, Dalian, China, 8876-8880

Gan Yong, Sun Yushan, Wan Lei, Pang Yongjie (2006). Motion control system of underwater robot without rudder and wing. *Proceeding of the 2006 IEEE International Conference on Intelligent Robotics and Systems*, Beijing, China, 3006-3011

Li Xuemin, Xu Yuru (2002). S-control of automatic underwater vehicles. *The Ocean Engineering*, 19(3), 81-84

Li Ye, Liu Jianchen, Shen Minxue (2005). Dynamics model of underwater robot motion control in 6 degrees of freedom. *Journey of Harbin Institute of Technology*, 12(4), 456-459

Ren Yongping, Li Shengyi (2005). Design method of a kind of new controller. *Control and Decision*, 20(4), 471-474

Venugopal KP, Sudhakar R (1992). On-line learning control of autonomous underwater vehicles using feedforward neural networks. *IEEE Journal of Oceanic Engineering*, 17(4), 308-319

Yuh J (1990). Modeling and control of underwater robotic vehicles. *IEEE Transaction on Systems, Man, and Cybernetics*, 20(6), 1475-1483

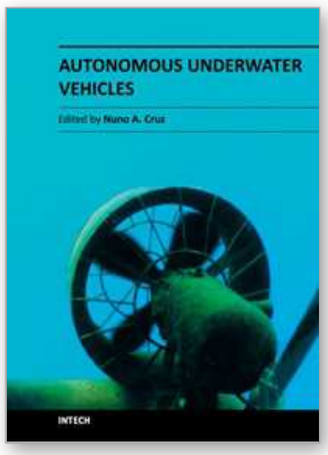

Autonomous Underwater Vehicles

Edited by Mr. Nuno Cruz

ISBN 978-953-307-432-0

Hard cover, 258 pages

Publisher InTech

Published online 17, October, 2011

Published in print edition October, 2011

Autonomous Underwater Vehicles (AUVs) are remarkable machines that revolutionized the process of gathering ocean data. Their major breakthroughs resulted from successful developments of complementary technologies to overcome the challenges associated with autonomous operation in harsh environments. Most of these advances aimed at reaching new application scenarios and decreasing the cost of ocean data collection, by reducing ship time and automating the process of data gathering with accurate geo location. With the present capabilities, some novel paradigms are already being employed to further exploit the on board intelligence, by making decisions on line based on real time interpretation of sensor data. This book collects a set of self contained chapters covering different aspects of AUV technology and applications in more detail than is commonly found in journal and conference papers. They are divided into three main sections, addressing innovative vehicle design, navigation and control techniques, and mission preparation and analysis. The progress conveyed in these chapters is inspiring, providing glimpses into what might be the future for vehicle technology and applications.

INTECH
open science | open minds

InTech Europe
University Campus STeP Ri
Slavka Krautzeka 83/A
51000 Rijeka, Croatia
Phone: +385 (51) 770 447
Fax: +385 (51) 686 166
www.intechopen.com

InTech China
Unit 405, Office Block, Hotel Equatorial Shanghai
No.65, Yan An Road (West), Shanghai, 200040, China
中国上海市延安西路65号上海国际贵都大饭店办公楼405单元
Phone: +86-21-62489820
Fax: +86-21-62489821

IntechOpen